Appl. Phys. A 74 [Suppl.], S1433–S1436 (2002) / Digital Object Identifier (DOI) 10.1007/s003390101241

Applied Physics A
Materials
Science & Processing

Engineering applications of Bragg-edge neutron transmission

J.R. Santisteban[1,*], L. Edwards[1], M.E. Fizpatrick[1], A. Steuwer[2], P.J. Withers[2]

[1] Department of Materials Engineering, The Open University, Milton Keynes MK7 6AA, UK
[2] Manchester Materials Science Centre, UMIST/University of Manchester, Grosvenor Street, Manchester M1 7HS, UK

Received: 18 July 2001/Accepted: 24 October 2001 –

Abstract. The shape, magnitude and location of the Bragg edges appearing in the transmission spectrum of polycrystalline materials can be accurately determined by the time-of-flight technique, and hence information about the stress state, texture and phases present in the material is readily available. An advantage of Bragg-edge transmission over conventional neutron diffraction is that it can use a pixellated detector to map the strain in plane samples, producing images analogous to neutron radiography. Moreover, maps of the unstressed lattice spacing can be achieved by tilting the sample relative to the direction of the neutron beam. Examples of the application of this technique to typical engineering problems are presented in this work.

PACS: 61.12.Ex; 83.85.Lq; 81.30.Mh

Neutron diffraction has proven to be a powerful tool to address potential industrial problems. The technique is commonly used for the determination of strains in materials and engineering components, as well as for real-time (or static) phase analysis. The weak interaction of neutrons with solids has opened up the possibility of monitoring precipitation of phases or internal strains non-destructively far inside the bulk material, even under working/loading conditions. In this work we show that many of these applications can also be accomplished by an analysis of the transmitted neutron beam using the time-of-flight technique (TOF). Moreover, we present two applications in which the transmission geometry has unique advantages over conventional neutron diffraction: (i) mapping of the unstressed lattice parameter and (ii) time-resolved phase transformations in simple structures.

A typical example of the Bragg edges appearing in the TOF spectrum of the transmitted neutrons is shown in Fig. 1. These Bragg edges occur because, for a given *hkl* reflection, the Bragg angle increases as the wavelength increases until 2θ is equal to 180°. At wavelengths greater than this critical value no scattering by this particular *hkl* lattice spacing can occur, and there is a sharp increase in the transmitted intensity. From Bragg's law the wavelength at which this occurs is $\lambda = 2d_{hkl}$, giving a measure of the *hkl* d-spacing in the direction of the incoming beam. We have developed a new edge profile function that allows a simple and very precise description of the Bragg edges observed at ISIS [1], as can be seen in the least-squares refinement shown in the inset of Fig. 1. This has enabled us to define interplanar distances in simple structures with a precision of $\Delta d/d = 10^{-5}$ in less than a minute.

1 Strain imaging

In neutron strain scanning the planes of atoms are used as internal strain gauges. Each Bragg edge corresponds to a particular lattice spacing for the crystal structure of the sample. A change in the position of a Bragg edge corresponds to a change in the lattice spacing for planes normal to the beam, and hence enables the determination of strain, $\varepsilon = (d^{hkl} - d_0^{hkl})/d_0^{hkl}$, in that direction. In practice, an average lattice parameter, a, is defined from a least-square refinement including many edges [2], providing a value closer to the macroscopic engineering strain [3]. The transmission geometry opens up the possibility of using an array of detectors to produce a radiographic "image" of the strain variation in the sample. However, it also means that the measurement is an average over the complete transmission path through the sample, making the method useful for examining plates and other essentially two-dimensional objects. With this in mind, a new pixellated detector consisting of a 10×10 array of 2×2 mm scintillator detectors on a 2.5-mm pitch has been developed [4]. An example of the use of this detector system involves measuring the strain around a cold expanded hole in a 12-mm-thick ferritic steel plate (Fig. 2). The fatigue lives of fastener holes may be increased if the hole is cold expanded prior to insertion of the fastener. The most common method presently used in the aircraft industry involves expansion of a lubricated split sleeve by an oversize mandrel using commercially available equipment. Fatigue-life predictions of structures containing such expanded holes rely criti-

*Corresponding author.
(Fax: +44-1908/653858, E-mail: j.r.santisteban@open.ac.uk)

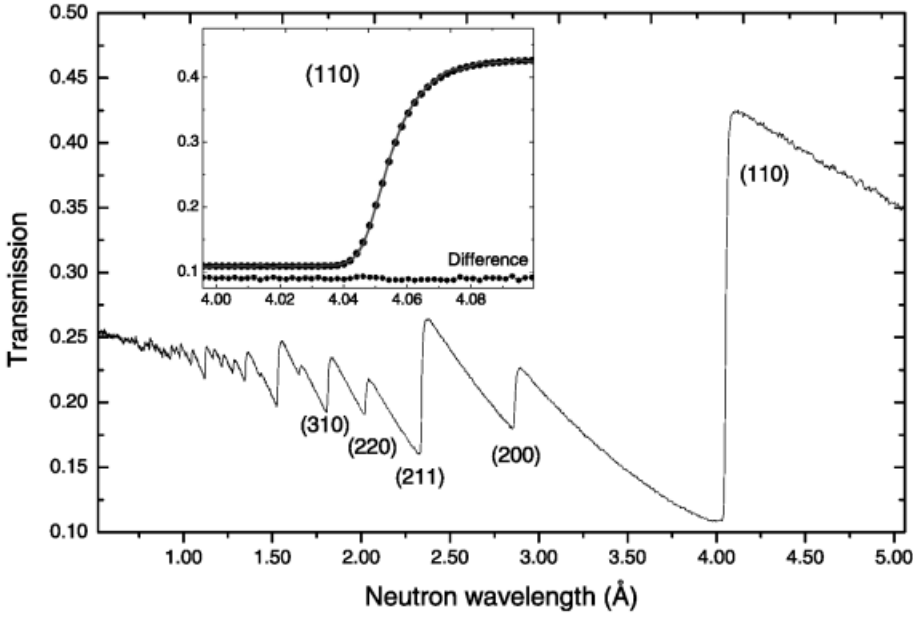

Fig. 1. Neutron transmission of Fe powder displaying characteristic Bragg edges. A least-squares refinement of the (110) edge is shown in the *inset*

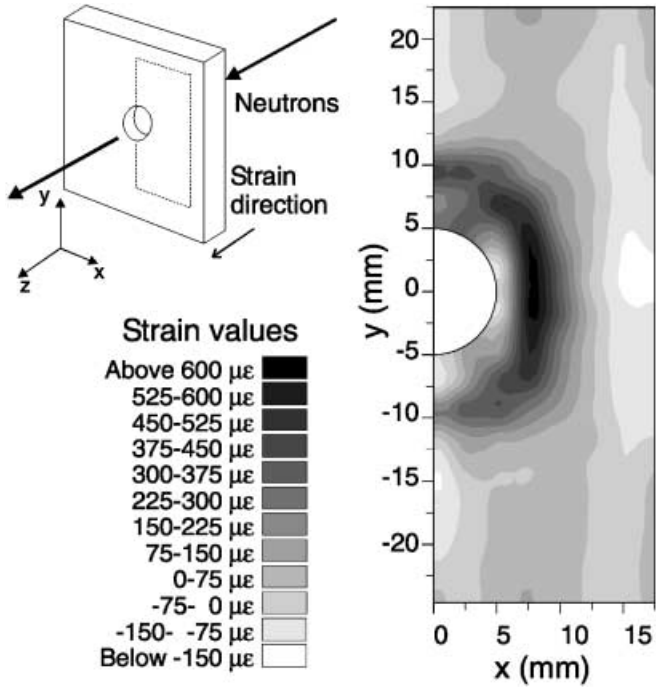

Fig. 2. Variation of the residual elastic strain in a cold expanded hole in a 12-mm-thick steel plate. The measured strains correspond to the through-thickness average of the out-of-plane strains

cally on estimates of the residual stress distribution surrounding the hole. The stress and strain distribution surrounding a cold expanded hole is therefore of significant engineering interest.

2 Unstressed lattice parameter

In any neutron diffraction experiment the problem of determining a stress-free lattice parameter (a_0) from which the elastic strains (and hence stresses) can be calculated remains difficult. In particular, in cases where there is a likelihood of compositional variation this problem presents a tremendous challenge to the reliability of the technique. This is extremely important for welds, where at the present time expensive component sectioning of the test-piece into small stress-free parts is required. The transmission technique can be used to produce a map of the stress-free lattice parameter across component slices [5]. For this purpose, we used the pixellated detector in combination with the so-called $\sin^2\psi$ technique [6]. For a plate specimen under a biaxial (plane) stress field, the unstressed lattice parameter can be defined from the shift observed in the position of the Bragg edges as the sample is tilted around two perpendicular axes, as shown in Fig. 3a. The linear dependence of the lattice parameter on $\sin^2\psi$ and the Poisson's ratio, ν, of the material univocally define a_0:

$$a_0 = a_\perp + \frac{\nu}{(1+\nu)}(m_{\mathrm{LD}} + m_{\mathrm{TD}})\,, \qquad (1)$$

where $a_\perp$ is the ordinate and m_{LD} and m_{TD} are the slopes observed when tilting in the longitudinal and transverse directions respectively. The value of a_0 is indicated by the dotted line in Fig. 3b. This method has been applied to produce a map of a_0 for a ferritic steel weld used as a round-robin sample in the VAMAS TWA 20 program. VAMAS TWA 20 is an international program charged with developing an international standard for non-destructive residual stress measurements by neutron diffraction. A thin slice (3-mm-thick) was machined from the weld, assuring the plane stress condition assumed in the method. A picture of the sample is shown in Fig. 3c, with the weld exposed by surface etching. By tilting the sample around longitudinal and transverse directions, a graph similar to Fig. 3b (but up to $\sin^2\psi = 0.22$) was produced for each point within the white rectangle. A map of a_0, expressed as pseudo-strain relative to the parent material, is shown in Fig. 3d. It is clear that the distribution of a_0 follows closely the shape of the weld. A difference as large as 600 με was found at the outermost weld caps.

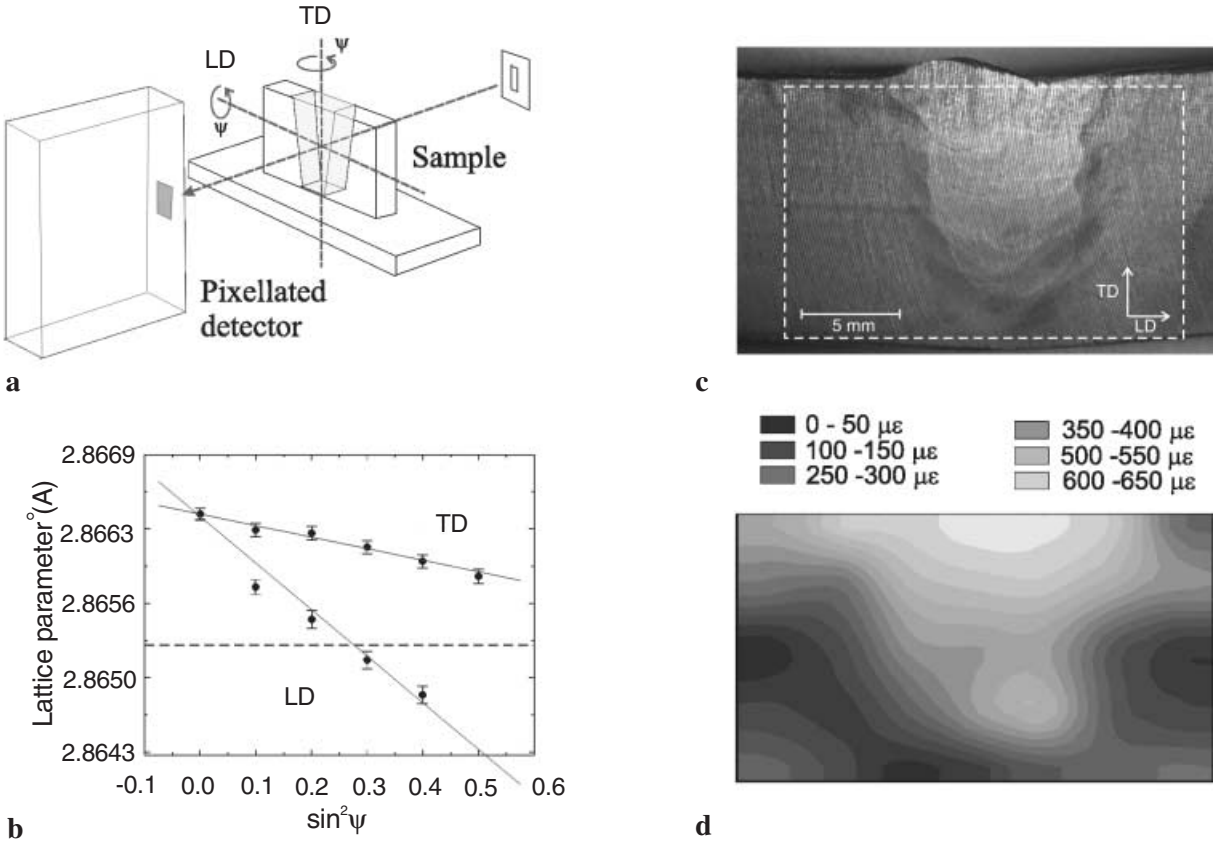

Fig. 3a–d. Determination of the unstressed lattice parameter, a_0, by transmission: **a** experimental setup, indicating the tilting angle ψ; **b** value of a_0 (*dotted line*) determined from the linear dependence of a on $\sin^2\psi$ for two orthogonal directions; **c** ferritic weld; and **d** a_0 map for the *white rectangle* shown in **c**, in terms of pseudostrain

3 In situ phase transformations

In addition to strain measurements, the very high counting rate obtained when summing all the pixels in the new detector opens new possibilities for the study of in situ phase transformations [7]. Moreover, the technique is not sensitive to the sample location along the beam, giving both high flexibility and relatively simple sample environments. Both advantages have been utilised in recent experiments designed to study the isothermal decomposition of austenite (fcc or γ-Fe) to bainite in a low alloy EN24 steel. (Bainite is essentially a mixture of ferrite (bcc α-Fe) and carbides.) EN24 is a high-

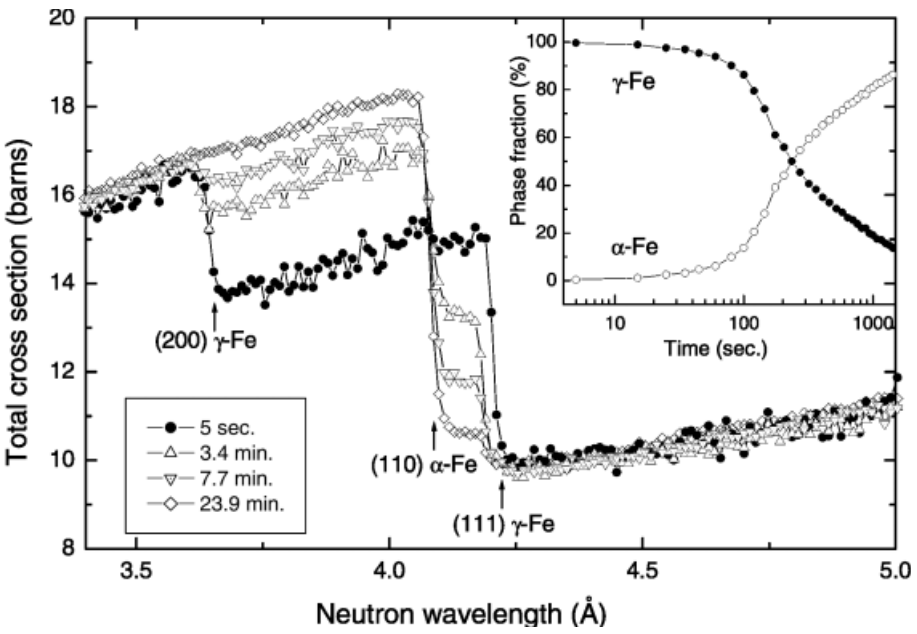

Fig. 4. Total cross-section of EN24 steel at 380 °C after austenisation at 830 °C. The times are measured from the time of insertion in the furnace. The *inset* shows the evolution of the phases, obtained after a Rietveld analysis of 32 spectra

strength engineering steel whose properties are critically dependent on heat treatment. Creation of a given property profile using differential heat treatment depends on reliable time–temperature–transformation (TTT) data describing the temporal evolution of it's constituent phases. The evolution of bainite in EN24 at 380 °C was studied using two tubular furnaces aligned with the neutron beam. After austenisation at 830 °C, the sample was moved into the 380 °C furnace after cooling with an air blast. All processes were performed in situ using counting times as short as 10 s. Figure 4 shows the total cross-section measured at four different times from insertion in the 380 °C furnace. The inset shows the time evolution of the γ and α phases, obtained after a Rietveld analysis of the transmission spectra using the code BetMan [8]. The value of the total cross-section for wavelengths beyond the first Bragg edge could be used to define the temperature of the sample.

4 Conclusions

The examples given here clearly show that unique information can be easily obtained from the transmitted neutron beam. In particular, by the use of a pixellated detector, a whole new range of applications involving the study of spatial distributions is ready to be unveiled.

References

1. J.R. Santisteban, L. Edwards, A. Steuwer, P.J. Withers: J. Appl. Cryst. **34**, 289 (2001)
2. A. Steuwer, P.J. Withers, J.R. Santisteban, L. Edwards, G. Bruno, M.E. Fitzpatrick, M.R. Daymond, M.W. Johnson, D.Q. Wang: Phys. Status Solidi A **185**, 221 (2001)
3. J.D. Kamminga, T.H. De Keijser, E.J. Mittemeijer, R. Delhez: J. Appl. Cryst. **33**, 1059 (2000)
4. J.R. Santisteban, L. Edwards, M.E. Fitzpatrick, A. Steuwer, P.J. Withers, M.R. Daymond, M.W. Johnson, N. Rhodes, E.M. Schooneveld: Nucl. Instrum. Methods A **481**, 255 (2002)
5. A. Steuwer, P.J. Withers, J.R. Santisteban, L. Edwards, M.E. Fitzpatrick, M.R. Daymond, M.W. Johnson, G. Bruno: Proc. Sixth Int. Conf. of Residual Stresses (IOM Communications, Oxford 2000)
6. I.C. Noyan, J.B. Cohen: *Residual Stress: Measurement by diffraction and interpretation* (Springer, Berlin, Heidelberg, New York 1987)
7. K. Meggers, H.G. Priesmeyer, W.G. Trela, M. Dahms: Mater. Sci. Eng. A **188**, 301 (1994)
8. S. Vogel: Ph.D. thesis, Kiel University (2000); available online at http://e-diss.uni-kiel.de